

Article

Discovery of highly potent inhibitors targeting the predominant drug-resistant S31N mutant of the influenza A virus M2 proton channel

Fang Li, Chunlong Ma, William F. DeGrado, and Jun Wang

J. Med. Chem., **Just Accepted Manuscript** • DOI: 10.1021/acs.jmedchem.5b01910 • Publication Date (Web): 15 Jan 2016

Downloaded from <http://pubs.acs.org> on January 19, 2016

Just Accepted

“Just Accepted” manuscripts have been peer-reviewed and accepted for publication. They are posted online prior to technical editing, formatting for publication and author proofing. The American Chemical Society provides “Just Accepted” as a free service to the research community to expedite the dissemination of scientific material as soon as possible after acceptance. “Just Accepted” manuscripts appear in full in PDF format accompanied by an HTML abstract. “Just Accepted” manuscripts have been fully peer reviewed, but should not be considered the official version of record. They are accessible to all readers and citable by the Digital Object Identifier (DOI®). “Just Accepted” is an optional service offered to authors. Therefore, the “Just Accepted” Web site may not include all articles that will be published in the journal. After a manuscript is technically edited and formatted, it will be removed from the “Just Accepted” Web site and published as an ASAP article. Note that technical editing may introduce minor changes to the manuscript text and/or graphics which could affect content, and all legal disclaimers and ethical guidelines that apply to the journal pertain. ACS cannot be held responsible for errors or consequences arising from the use of information contained in these “Just Accepted” manuscripts.

1
2
3
4
5
6
7
8
9
10
11
12
13
14
15
16
17
18
19
20
21
22
23
24
25
26
27
28
29
30
31
32
33
34
35
36
37
38
39
40
41
42
43
44
45
46
47
48
49
50
51
52
53
54
55

Discovery of highly potent inhibitors targeting the predominant drug-resistant S31N mutant of the influenza A virus M2 proton channel

Fang Li,^{†,‡} Chunlong Ma,^{†,‡} William F. DeGrado,[§] Jun Wang^{*,†,‡}

[†]Department of Pharmacology and Toxicology, College of Pharmacy, The University of Arizona, Tucson, Arizona 85721, United States

[‡]BIO5 Institute, The University of Arizona, Tucson, Arizona, 85721, United States

[§]Department of Pharmaceutical Chemistry, University of California, San Francisco, California 94158, United States

* Corresponding author:

Jun Wang, Tel: 520-626-1366, Fax: 520-626-0749, email: junwang@pharmacy.arizona.edu

56
57
58
59
60

KEYWORDS. Influenza A virus, M2 proton channel, M2-S31N inhibitor

ABSTRACT

1
2
3
4
5
6
7
8
9
10
11
12
13
14
15
16
17
18
19
20
21
22
23
24
25
26
27
28
29
30
31
32
33
34
35
36
37
38
39
40
41
42
43
44
45
46
47
48
49
50
51
52
53
54
55
56
57
58
59
60

With the emergence of highly pathogenic avian influenza (HPAI) H7N9 and H5N1 strains, there is a pressing need to develop direct-acting antivirals (DAAs) to combat such deadly viruses. The M2-S31N proton channel of the influenza A virus (A/M2) is one of the validated and most conserved proteins encoded by the current circulating influenza A viruses, thus it represents a high-profile drug target for therapeutic intervention. We recently discovered a series of S31N inhibitors with the general structure of adamantyl-1-NH₂⁺CH₂-aryl, but they generally had poor physical properties and some showed toxicity *in vitro*. In this study, we sought to optimize both the adamantyl as well as the aryl/heteroaryl group. Several compounds from this study exhibited submicromolar EC₅₀ values against S31N-containing A/WSN/33 influenza viruses in antiviral plaque reduction assays with a selectivity index greater than 100, indicating that these compounds are promising candidates for in depth preclinical pharmacology.

INTRODUCTION

Influenza virus infections are a major global health threat. Despite the availability of influenza vaccines and small molecule antivirals, an estimated 10–15% of the population is infected annually in the United States,¹ leading to approximately 36,000 deaths and 200,000 hospitalizations.^{2, 3} Currently, vaccination remains the most effective way to prevent influenza virus infection; however, it is only partially effective and offers 65% protection in the best scenario.⁴ Moreover, due to the antigenic shift and drift of influenza viruses, influenza vaccines have to be regenerated every year.^{5, 6} Even though more effective broad-neutralizing antibodies are still in development,⁷⁻⁹ there is an immediate need for small molecule drugs, particularly for combating emerging highly pathogenic influenza strains, such as H5N1 and H7N9 for which vaccines were not immediately available in the first few months of influenza outbreak. These highly pathogenic avian influenza strains might become human-to-human transmissible with just a few additional mutations.¹⁰ Thus, small molecule antivirals that target the most conserved viral proteins, such as the A/M2 proton channel, are highly desired.^{11, 12}

A/M2 is a viral membrane protein that forms a homotetrameric proton-selective channel in the viral envelope.^{13, 14} The recognized function of A/M2 includes acidifying the viral interior after endocytosis, thereby initiating viral uncoating. In certain strains of influenza A viruses, A/M2 also functions to equilibrate the pH across the lumen of the late Golgi apparatus, thus preventing premature conformational change of the viral fusogenic protein-hemagglutinin.¹⁵

Interest in understanding the proton conductance and drug inhibition mechanism of A/M2 has been strongly motivated by its involvement in influenza virus infections.¹⁴ A/M2 was first discovered as the protein target of the anti-influenza drug amantadine.^{16, 17} However, the use of

1
2
3 amantadine was discontinued due to the prevalence of drug-resistant mutants.¹⁸ Among the large
4
5 number of drug-resistant mutants identified in cell culture and amantadine-treated patients, only
6
7 three major mutants, namely V27A, L26F, and S31N, have been found in transmissible viruses.^{19,}
8
9
10
11 ²⁰ The stringency of sequence conservation in M2 reflects tight functional constraints on the
12
13 pore-lining residues, where a single mutation to a monomer in M2 causes four changes within
14
15 the highly constricted pore.¹³ This small set of transmissible mutants suggests that M2 is a highly
16
17 conserved drug target compared with other viral proteins, rendering it an ideal drug target for the
18
19 development of anti-influenza drugs.²¹ However, drug discovery targeting M2 has been
20
21 hampered by the lack of a reliable high-throughput screening assay and high-resolution
22
23 structures. Nevertheless, guided by information gathered from molecular dynamics simulations,^{22,}
24
25
26
27 ²³ X-ray crystallography,^{24, 25} solution- and solid-state NMR spectroscopy,^{22, 26, 27} recent years
28
29 have witnessed significant progress in this area, and several classes of compounds have been
30
31 shown to inhibit all three major drug resistant mutants: V27A, L26F, and S31N.^{22, 27-31}
32
33
34 Subsequently, through iterative cycles of modeling, medicinal chemistry, electrophysiological
35
36 testing, and antiviral assaying, the potencies of several lead compounds were further improved to
37
38 the point where their IC₅₀ values against drug-resistant M2 mutants were better than that of
39
40 amantadine in inhibiting the wild-type M2 channel (Figure 1). The general structure of an S31N
41
42 inhibitor contains adamantyl-1-NH₂⁺CH₂-Aryl.^{27, 31} In this study, we systematically explored
43
44 various hydrophobic scaffolds and substituted-adamantanes as replacements of adamantane and
45
46 examined several other heterocycles as the aryl headgroup. This study resulted in several
47
48
49
50
51
52
53
54
55
56
57
58
59
60

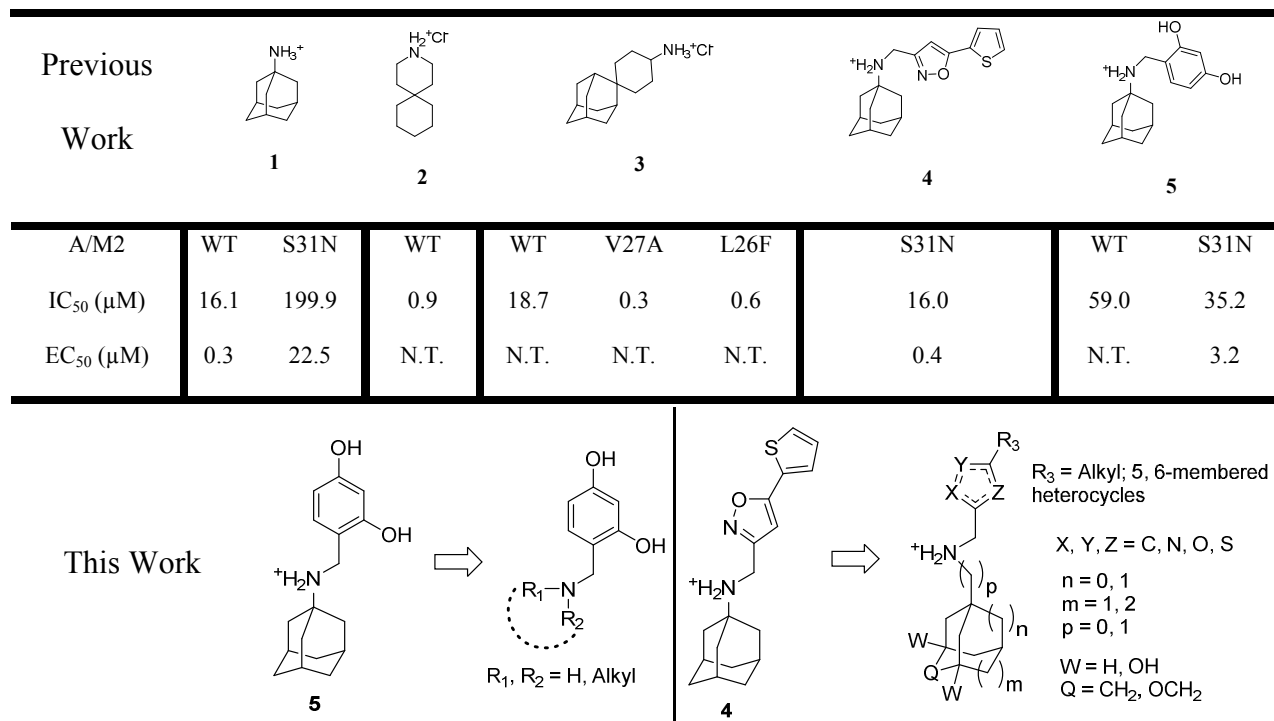


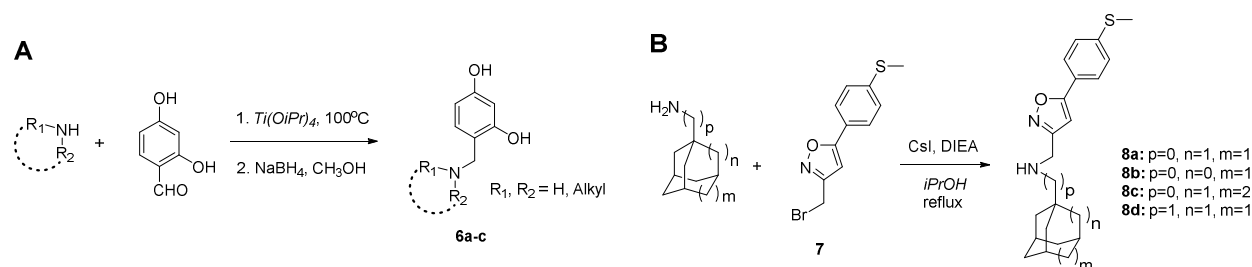
Figure 1. Chemical structures of inhibitors targeting the drug-resistant influenza A virus M2 proton channels, V27A, L26F, and S31N, and the SAR of S31N inhibitors explored in this study. IC₅₀ values were determined in two-electrode voltage clamp assays. EC₅₀ values were determined from plaque reduction assays. A/Udorn/72, A/Udorn/72-V27A, and A/WSN/33 influenza strains were used in plaque reduction assays for determining drug sensitivity to WT, V27A, and S31N inhibitors, respectively. N.T. = not tested.

RESULTS AND DISCUSSION

CHEMISTRY

The synthetic routes to compounds with various hydrophobic scaffolds, **6a–c** and **8a–d**, are shown in Scheme 1. The synthesis of the adamantyl-benzyl series of compounds was carried out by reductive amination of amines with 2,4-dihydroxybenzaldehyde (Scheme 1A).³¹ The isoxazole series of compounds was synthesized by direct alkylation (Scheme 1B).²⁷

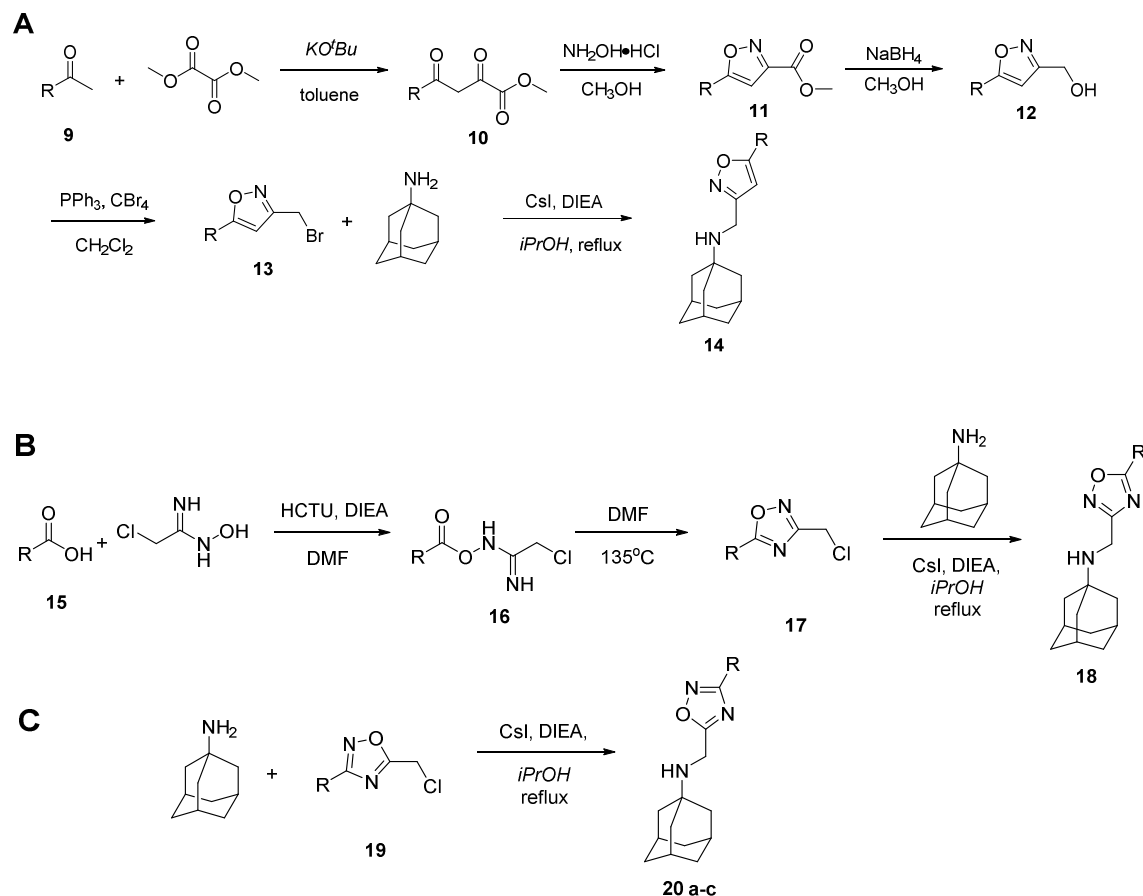
Scheme 1. Synthetic routes to M2 inhibitors bearing various hydrophobic scaffolds.



Synthesis of compounds **14** with various substitutions at the 5 position of isoxazole is shown in Scheme 2A.³² The synthesis started with a condensation reaction of methyl ketone **9** and dimethyl oxalate using potassium *tert*-butoxide as the base (Scheme 2A). Subsequent cyclization with hydroxylamine hydrochloride under mild heating at 50 °C in CH₃OH gave the isoxazole ester intermediate **11**. Yields for these two steps range from 61% to 82%. The ester was next reduced to the alcohol **12** by addition of sodium borohydride and converted to bromide **13** by triphenyl phosphine and carbon tetrabromide in dichloromethane. Overall yields for these two steps are 68–83%. Bromination using PPh₃ and CBr₄ significantly improved the yield compared to phosphorous tribromide.²⁷ The final N-alkylation of amantadine was performed under refluxing condition in isopropanol with cesium iodide as the catalyst and triethyl amine as the base in yields ranging from 62% to 91%.

The synthesis of compound **18** bearing 1,2,4-oxadiazole is shown in Scheme 2B.³³ Condensation of carboxylic acid **15** with 2-chloro-N-hydroxyethanimidamide gave the hydroxylamine ester **16**, which was cyclized under heating in DMF to give the oxadiazole methylene chloride **17**. Subsequent N-alkylation gave oxadiazole analogs **18** with 30–65% overall yields. 1,2,4-oxadiazoles (**20a–c**) with the adamantylamino methylene at the 5 position were synthesized by alkylation (Scheme 2C).

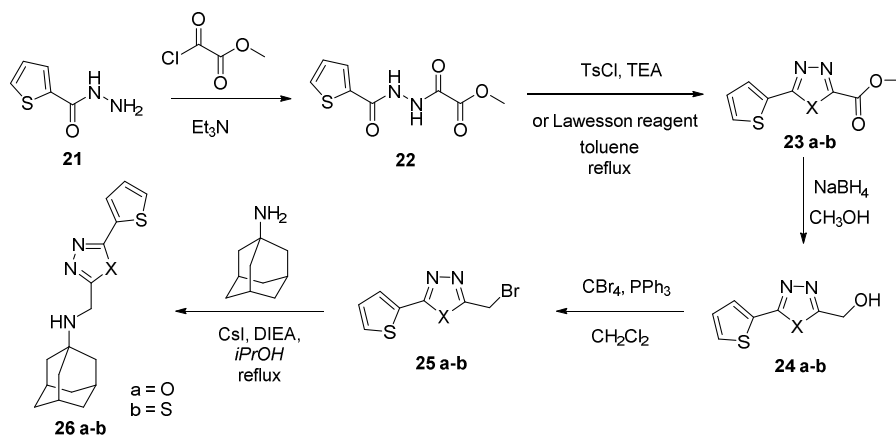
Scheme 2. Synthetic routes to adamantane derivatives bearing an isoxazole or oxadiazole headgroup.



The synthesis of 1,3,4-oxadiazole and 1,3,4-thiadiazole compounds **26a,b** is shown in Scheme 3.³⁴ Treatment of the 2-thiophenecarboxylic acid hydrazide **21** with methyl oxalyl chloride gave methyl 2-oxo-2-(thiophen-2-ylformohydrazido)acetate **22** in nearly quantitative yield. This intermediate (**22**) was cyclized upon treatment with *p*-toluenesulfonyl chloride (TsCl) or Lawesson's reagent to give 1,3,4-oxadiazole ester **23a** and 1,3,4-thiadiazole ester **23b**, respectively.³⁴ The yields for **23a** and **23b** were 80% and 75%, respectively. The esters were subsequently reduced to hydroxyl **24**, followed by bromination and alkylation to give the final compounds **26a,b**. Other 1,3,4-oxadiazole analogs **26c,d** and thiazoles **26e-j** were synthesized by

reductive amination or alkylation using commercially available aldehydes and halides as shown in Scheme 1.²⁷

Scheme 3. Synthetic route to adamantane derivatives bearing 1,3,4-oxadiazole or 1,3,4-thiadiazole headgroup.

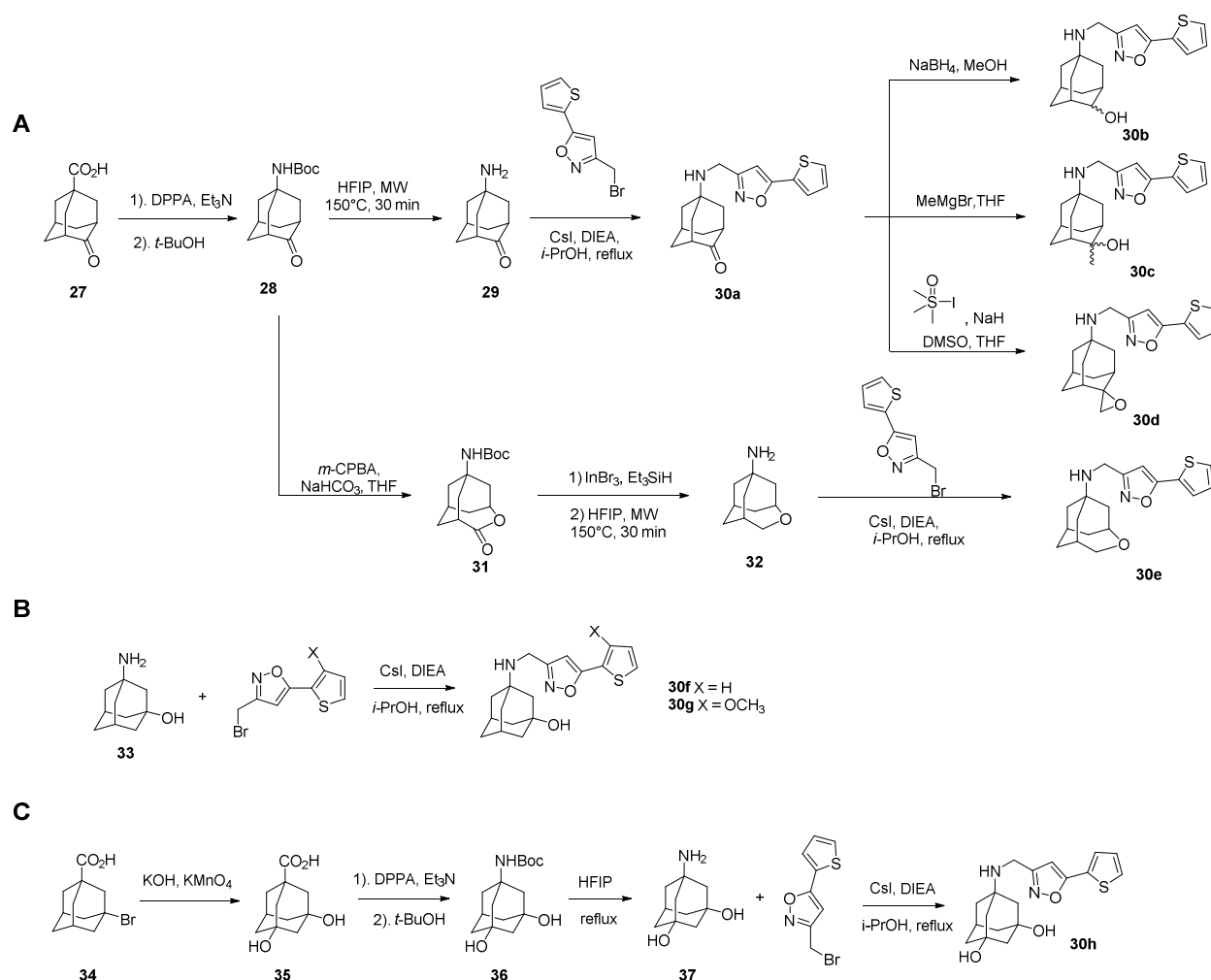


Compounds with substituted-adamantanes or adamantane analogs as the hydrophobic scaffolds were synthesized from a common precursor, 4-oxoadamantane-1-carboxylic acid (**27**) (Scheme 4A). One-pot Curtius rearrangement followed by treatment with *tert*-butanol gave *tert*-butyl N-(4-oxoadamantan-1-yl)carbamate (**28**) in 78% yield.³⁵ Subsequent deprotection with hexafluoroisopropanol (HFIP) under microwave irradiation gave 5-aminoadamantan-2-one (**29**). Alkylation of **29** with 3-(bromomethyl)-5-(thiophen-2-yl)-1,2-oxazole gave the key intermediate **30a** in 75% yield. The ketone in **30a** was next either reduced by NaBH₄ or alkylated by MeMgBr, or oxidized by the in situ-generated Corey-Chaykovsky reagent³⁶ to give **30b**, **30c**, and **30d**, respectively.

The ring-expanded 4-oxatricyclo [4.3.1.1^{3,8}]undecan-1-amine (**32**) was synthesized by Baeyer-Villiger oxidation of **28** with *meta*-chloroperoxybenzoic acid (*m*CPBA), followed by reduction with indium bromide and triethylsilane and deprotection with HFIP. Finally, installation of the 5-

(thiophen-2-yl)-1,2-oxazole was achieved through alkylation using CsI and DIEA under reflux condition in isopropanol to give **30e** in 27% overall yield. Compounds **30f,g** were synthesized through the same alkylation procedure starting from 3-aminoadamantan-1-ol (**33**). Compound **30h** with 3,5-dihydroxyl adamantane was synthesized from 3-bromo-1-adamantanecarboxylic acid (**34**). Oxidation of **34** using KMnO_4 gave 3,5-dihydroxyl-1-adamantanecarboxylic acid (**35**). Subsequent Curtius rearrangement followed by treatment with *tert*-butanol gave **36**. Next deprotection of **36** followed by alkylation afforded the final compound **30h**. The overall yield was 17%.

Scheme 4. Synthetic route to M2-S31N inhibitors bearing adamantane analogs



STRUCTURE–ACTIVITY RELATIONSHIP (SAR) STUDY

Exploring the hydrophobic scaffold as a replacement for adamantane in S31N inhibitors.

Our previous studies of the S31N inhibitors revealed two classes of potent S31N inhibitors (**4** and **5**), both of which share the same general structure of adamantyl-1-NH₂⁺CH₂-aryl (Figure 1).^{27, 31} The adamantyl-benzyl series of compounds, a representative example of which is compound **5**, are active against both the WT and the S31N mutant of M2,³¹ while the adamantyl-isoxazole series, such as **4**, show selective inhibitory against S31N.²⁷ SAR studies of the adamantyl-benzyl series revealed that the –NH₂⁺CH₂– linker is essential for this activity.³¹ However, the adamantyl scaffold has not been explored. It has been shown that inhibitors with a wide variety of hydrophobic scaffolds, such as linear alkyl, mono-cyclic alkyl, bi-cyclic alkyl, and spiro-alkyl, are potent channel blockers of the WT M2.^{28, 37-41} Thus we sought to explore various hydrophobic scaffolds in both series of S31N inhibitors and examine how this modification would affect their inhibition against both WT and S31N. The hydrophobic scaffolds include adamantane analogs such as ring-contracted adamantane (**6a**, **8b**), ring-expanded adamantane (**6b**, **8c**), and spiroamine (**6c**) (Table 1). All of the hydrophobic scaffolds examined (without aryl headgroup) are potent inhibitors against WT-M2.³⁷

The synthesized compounds were first tested in two-electrode voltage clamp (TEVC) electrophysiological assays, in which M2 was expressed in *Xenopus laevis* oocytes and current conductance across cell membrane was recorded in a whole cell format.²⁹ All compounds were initially tested at 100 μM drug concentration against both WT and S31N. The antiviral activity of potent compounds with greater than 80% M2 channel inhibition at 100 μM in TEVC assays were further confirmed in plaque reduction assays. For the 2,4-dihydroxyl benzyl series of compounds, replacing the adamantane scaffold in **5** with noradamantane (**6a**), aza-adamantane (**6b**) or

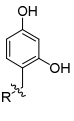
1
2
3
4
5
6
7
8
9
10
11
12
13
14
15
16
17
18
19
20
21
22
23
24
25
26
27
28
29
30
31
32
33
34

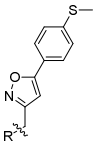
spiropiperidine substituent (**6c**) decreased the M2-S31N channel blockage (Table 1). However, the resulting compounds (**6a–c**) all displayed similar or higher inhibitory activity against WT-M2. Similar SAR was also observed for the isoxazole series of compounds: replacing the adamantane in **8a** with other hydrophobic scaffolds ameliorated activity against S31N, and all compounds in this series (**8a–d**) remained inactive against WT. Insertion of a methylene linker between the adamantyl and ammonium gave **8d**, which is significantly less active than the parent compound **8a** in inhibiting the S31N channel. Collectively, adamantane (**5** and **8a**) and ring-expanded adamantane (**8c**) appeared to be the optimal hydrophobic scaffolds for S31N inhibition, while a wide variety of hydrophobic scaffolds are tolerated for WT-M2 inhibition. Noradamantane scaffold was also tolerated for S31N inhibition, although corresponding compounds (**6a** and **8b**) were less active than their adamantane counterparts. A secondary amine group appeared to be essential for S31N inhibition as compounds with a tertiary amine (**6b** and **6c**) were completely inactive.

35
36
37

Table 1. Exploring various hydrophobic scaffolds in S31N inhibitors

38
39
40
41
42
43
44
45
46
47
48
49
50
51
52
53
54
55
56
57
58
59
60

	R	Compound ID	%S31N inhibition*	%WT inhibition*
		AMT (1)	36	91
		5	67	64

		6a	40	64
		6b	0	74
		6c	3	65
		8a	79	5
		8b	71	19
		8c	75	11
		8d	34	14

*Values represent the mean of three independent measurements. We typically see no more than 5% variation in the percent inhibition on a given day, or 10% error for measurements made on different days with different batches of oocytes. Data listed is percent inhibition when tested at 100 μ M drug concentration. N.T. = Not tested.

Exploring hydrophobic substitutions of isoxazole and 1,2,4-oxadiazole. Solution NMR structure of **4** bound to M2-S31N (19–49) shows the distal thienyl ring of the drug forms

hydrophobic interactions with V27 side chain methyl groups (Figure 2),²⁷ suggesting that other hydrophobic alkane substituents can be similarly accommodated at the same position.

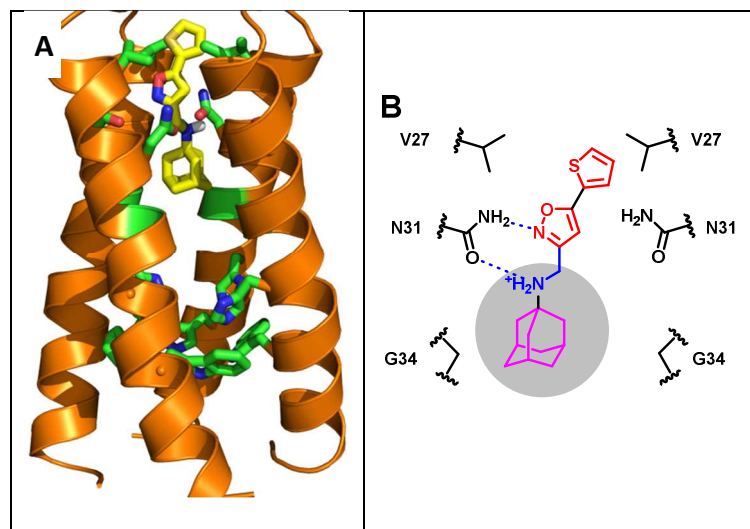
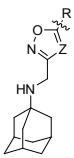


Figure 2. Drug binding mode of the A/M2-S31N mutant. (a) Solution NMR structure of A/M2-S31N bound with the isoxazole inhibitor-M2WJ332 (**4**) (PDB: 2LY0). (b) Representation of drug-protein interactions.

Replacing a small methyl substituent at the 5 position of isoxazole or 1,2,4-oxadiazole (**14a** and **18a**) with a bulkier propyl (**14b** and **18b**), cyclopropyl (**14c** and **18c**), isopropyl (**14f** and **18d**), cyclobutyl (**14d**), or 2-methyl-2-(methylsulfanyl)propyl (**14g**) group dramatically increased the activities against S31N. Compound **14e** with a terminal methoxy group was much less active than its methylene analog **14b**, highlighting the importance of hydrophobic interactions with the V27 side chains in high-affinity binding of drugs. Increasing the size of the substituent from isopropyl (**18d**) to isobutyl (**18e**), however, led to a slight decrease in S31N inhibition. The most active compound against S31N in this series is **14h**, showing 90% inhibition at 100 μ M. In general, isoxazole-containing compounds are more active than 1,2,4-oxadiazole-containing analogs. It was also noticed that increasing the size of the substituents at the 5 position of isoxazole and oxadiazole decreased their inhibition against WT M2. The active compounds were

further tested in plaque reduction assays against S31N-containing A/WNS/33 viruses, and two compounds, **14c** and **14d**, were found to decrease the plaque number more than 50% at 1 μ M, indicating their EC₅₀ values are less than 1 μ M.

Table 2. Exploring hydrophobic substitutions of isoxazole and 1,2,4-oxadiazole

	R	Z	Compound ID	% S31N inhibition*	% WT inhibition*	% plaque formation at 1 μ M (A/WSN/33)**
		C	14a ^a	49/N.T.	55	N.T.
		N	18a ^a	60/N.T.	41	N.T.
		C	14b	81/49	16	73 \pm 7
		N	18b	77/19	19	N.T.
		C	14c ^a	85/65	19	42 \pm 3
		N	18c ^a	81/60	18	82 \pm 5
		C	14d	84/N.T.	30	42 \pm 2
		C	14e	39/N.T.	18	N.T.
		C	14f	80/55	18	66 \pm 2
		N	18d ^a	70/N.T.	10	N.T.
		N	18e	62/N.T.	12	N.T.
	C	14g	70/N.T.	14	N.T.	
	C	14h	90/N.T.	13	57 \pm 2	

*Values represent the mean of three independent measurements. We typically see no more than 5% variation in the percent inhibition on a given day, or 10% error for measurements made on different days with different batches of oocytes. All compounds were initially tested at 100 μ M. Compounds that showed greater than 80% inhibition at 100 μ M were further tested at 30 μ M. The data are presented as percent inhibition at 100 μ M/percent inhibition at 30 μ M. N.T. = Not

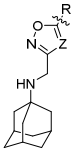
1
2
3 tested. ^a Percent inhibition in TEVC assays was previously reported. ^{**} Plaque reduction assays
4
5 were performed against the M2-S31N containing A/WSN/33 virus in duplicates; percent of
6
7 plaque formation is defined as the ratio of plaque numbers in the presence of compounds divided
8
9 by the plaque numbers in the absence of compounds.
10
11

12 13 14 15 **Exploring substitutions in the distal aromatic ring of isoxazole and 1,2,4-oxadiazole**

16
17
18 It has been found that S31N inhibition is relatively insensitive to different regioisomers of the
19
20 distal ring at the 5 position of isoxazole and 1,2,4-oxadiazole: compounds **14i** and **18g** showed
21
22 similar activities as **4** and **18f**, respectively. This finding suggests that the sulfur atom in the
23
24 distal thienyl ring is not involved in specific interactions with the M2 channel, which is
25
26 consistent with the solution NMR structure showing that the thienyl group of **4** forms
27
28 hydrophobic interactions with the Val27 side chain methyls.²⁷ Compounds with a furanyl
29
30 substitution, **14j** and **18h**, were slightly less active, which might due to decreased hydrophobicity
31
32 (the clogP for **4** and **14j** is 3.74 and 2.37, respectively, as calculated from ChemBioDraw 14).
33
34 Compound **14k** with a methoxyl at the 3 position of the distal thienyl ring was highly active
35
36 against S31N, showing 87% inhibition at 30 μM. When a phenyl ring was placed at the 5
37
38 position of isoxazole and 1,2,4-oxadiazole, the S31N inhibition of the resulting compounds, **14l**
39
40 and **18i**, was retained. Halogen substitution in the distal phenyl ring was also examined, and the
41
42 S31N inhibition was found to be insensitive to these structural modifications. All chloro-
43
44 substituted (**14m** and **18j**), bromo-substituted (**14n**), and difluoro-substituted (**14o** and **14p**)
45
46 compounds showed similar potency as **14l** and **18i**. Mono-methoxyl substitution at all three
47
48 positions of the phenyl ring, ortho (**18l**), meta (**14r**), and para (**14q** and **18k**), did not affect the
49
50 S31N inhibition. Similarly, compounds with mono-methylsulfanyl substitutions at the ortho (**14s**)
51
52
53
54
55
56
57
58
59
60

and para (**14a**) of the distal phenyl ring retained potent inhibition against S31N. Double-methoxyl substitutions decreased the S31N inhibition of the isoxazole-containing compound **14t**, but not the 1,2,4-oxadiazole-containing compound **18m**. Consistent with previous SAR conclusions, compounds with 1-(1-adamantylamino)-methylene substitution were more active when placed at the 3 position of isoxazole and 1,2,4-oxadiazole than at the 5 position (**20b** versus **18l**, **20c** versus **14h**).²⁷ In plaque reduction assays, several compounds, **14k**, **14l**, and **14r**, showed comparable or even better antiviral activity than the parent compound **4** in inhibiting A/WSN/33 virus replication.

Table 3. Exploring aromatic substitutions of isoxazole and 1,2,4-oxadiazole

	R	Z	Compound ID	% S31N inhibition*	% WT inhibition*	% plaque formation at 1 μM (A/WSN/33)**
		C	4 ^a	90/63	11	32±2
		N	18f ^a	83/N.T.	11	66±3
		C	14i	90/N.T.	28	47±5
		N	18g	81/N.T.	3	74±10
		C	14j	84/N.T.	12	47±1
		N	18h	73/N.T.	24	N.T.
		C	14k	90/87	27	39±3
		C	14l ^a	91/N.T.	20	26±3
		N	18i ^a	75/N.T.	8	N.T.
		C	14m	87/65	14	84±6
		N	18j	86/72	16	88±1
		C	14n	77/N.T.	12	N.T.
		C	14o	78/N.T.	23	N.T.

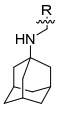
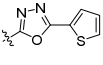
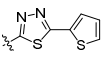
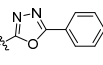
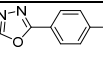
		C	14p	85/68	8	56±7
		C	14q^a	87/N.T.	13	59±9
		N	18k^a	86/N.T.	18	92±7
		C	14r	87/73	12	39±1
		C	14s	79/N.T.	8	N.T.
		C	8a	79/N.T.	5	N.T.
		N	18l	90/77	7	66±3
		C	14t	62/N.T.	10	N.T.
		N	18m	82/N.T.	18	76±5
		N	20a	39/N.T.	18	N.T.
		N	20b	58/N.T.	13	N.T.
		C	20c	67/N.T.	27	N.T.

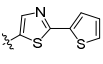
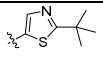
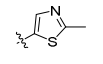
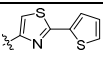
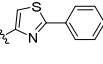
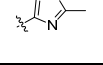
*Values represent the mean of three independent measurements. We typically see no more than 5% variation in the percent inhibition on a given day, or 10% error for measurements made on different days with different batches of oocytes. The data are presented as percent inhibition at 100 μ M/percent inhibition at 30 μ M. N.T. = Not tested. ^aPercent inhibition in TEVC assays was previously reported. ^{**}Plaque reduction assays were performed against the M2-S31N containing A/WSN/33 virus in duplicates. The percent of plaque formation is defined as the ratio of plaque numbers in the presence of compounds divided by the plaque numbers in the absence of compounds.

Exploring 1,3,4-oxadiazole-, 1,3,4-thiadiazole-, and thiazole-containing M2 inhibitors

To investigate whether isoxazole and 1,2,4-oxadiazole can be replaced by other heterocycles, several 1,3,4-oxadiazole-containing compounds (**26a**, **26c**, and **26d**) were synthesized. All three 1,3,4-oxadiazole-containing compounds were less active than their isoxazole and 1,2,4-oxadiazole counterparts (**26a** versus **4** and **18f**; **26c** versus **14l** and **18i**; **26d** versus **14q** and **18k**). Encouragingly, a 1,3,4-thiadiazole-containing compound, **26b**, was similarly active as the isoxazole analog (**4**) in both TEVC and plaque reduction assays. **26b** also showed no apparent toxicity up to 200 μM . Compound **26e** with a 1-(1-adamantylamino)-methylene substitution at the 5 position of thiazole was also potent, showing 75% inhibition at 100 μM concentration. Replacement of the distal thienyl ring at the 2 position of thiazole in **26e** with methyl (**26g**) and tert-butyl (**26f**) dramatically decreased S31N inhibition. Compounds containing another thiazole regioisomer with 1-(1-adamantylamino)-methylene at the 4 position of thiazole were much less active. All compounds were found to have minimal inhibition against WT M2, except **26j** (57% inhibition at 100 μM).

Table 4. Exploring 1,3,4-oxadiazole, 1,3,4-thiadiazole, and thiazole

	R	Compound ID	% S31N inhibition*	% WT inhibition*	% plaque formation at 1 μM (A/WSN/33)**	CC ₅₀ (μM)
		26a	52/N.T.	16	N.T.	N.T.
		26b	83/N.T.	21	39 \pm 2	>200
		26c	61/N.T.	18	N.T.	N.T.
		26d	58/N.T.	3	N.T.	N.T.

	26e	75/N.T.	13	N.T.	113
	26f^a	38/N.T.	5	N.T.	N.T.
	26g^a	28/N.T.	22	N.T.	N.T.
	26h	37/N.T.	7	N.T.	N.T.
	26i	24/N.T.	0	N.T.	N.T.
	26j^a	36/N.T.	57	N.T.	N.T.

*Values represent the mean of three independent measurements. We typically see no more than 5%

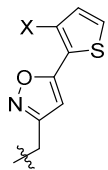
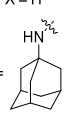
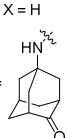
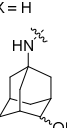
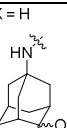
variation in the percent inhibition on a given day, or 10% error for measurements made on different days with different batches of oocytes. The data are presented as percent inhibition at 100 μ M/percent inhibition at 30 μ M. N.T. = Not tested. ^a Percent inhibition in TEVC assays was previously reported. **Plaque reduction assays were performed against the M2-S31N containing A/WSN/33 virus in duplicates. The percent of plaque formation is defined as the ratio of plaque numbers in the presence of compounds divided by the plaque numbers in the absence of compounds.

Exploring adamantane analogs as potent M2 inhibitors

Having identified the favorable aryl auxiliary substitutions on M2-S31N inhibitors, we decided to revisit the hydrophobic scaffolds. Our preliminary data suggested adamantane is the optimal scaffold for S31N inhibition; we therefore focused on substituted adamantanes, such as 4-hydroxyl adamantane (**30b**), 3-hydroxyl adamantane (**30f,g**), 3,-5-dihydroxyl adamantane (**30h**), 4-hydroxyl-4-methyl adamantane (**30c**), spiro[adamantane-2,2'-oxirane] (**30d**), and 4-oxatricyclo[4.3.1.1^{3,8}]undecane (**30e**). 5-(thiophen-2-yl)-1,2-oxazole and 5-(3-methoxythiophen-

2-yl)-1,2-oxazole were chosen as the aryl auxiliary substitutions as they are among the most favorable aryl substitutions for S31N inhibition. Compared with the parent compound **4**, all modifications except **30d** retained potent channel blockage against M2-S31N, showing more than 70% inhibition at 100 μM . In plaque reduction assays, compounds with hydroxylation on the adamantane ring, **30b**, **30f**, and **30g**, were similarly potent as the parent compound **4**, all showing EC_{50} s less than 1 μM (Figure 3). However, further increasing the hydrophilicity by adding an additional hydroxyl group led to a significant loss of activity (compound **30h** versus compound **30f**). Notably, hydroxylation of the adamantane ring greatly decreased the cellular cytotoxicity of the parent compound (compound **30f** versus compound **4**).

Table 5. Exploring adamantane analogs as the hydrophobic scaffolds

	X, R	Compound ID	% S31N inhibition*	% plaque formation at 1 μM **	Plaque Reduction EC_{50} (μM)**	CC_{50} (μM)***	clogP^{Δ}
	X = H R = 	4	90	32 \pm 2	0.353	100	4.2
	X = H R = 	30a	78/N.T.	31 \pm 1	N.T.	N.T.	2.6
	X = H R = 	30b	91/56	10 \pm 3	0.727	116	2.1
	X = H R = 	30c	87/48	27 \pm 2	N.T.	N.T.	2.6

1 2 3 4 5 6 7 8		30d	61/N.T.	72±3	N.T.	N.T.	2.5
9 10 11 12 13		30e	72/N.T.	58±1	N.T.	N.T.	2.8
14 15 16 17 18		30f	82/N.T.	40±1	0.510	>200	2.7
19 20 21 22 23		30g	86/N.T.	33±2	0.404	N.T.	2.2
24 25 26 27 28 29		30h	88/45	69±4	2.5	>200	2.0

30
31
32
33
34
35
36
37
38
39
40
41
42
43
44
45
46
47
48
49
50
51
52
53
54
55
56
57
58
59
60

*Values represent the mean of three independent measurements. We typically see no more than 5% variation in the percent inhibition on a given day, or 10% error for measurements made on different days with different batches of oocytes. The data are presented as percent inhibition at 100 μ M/percent inhibition at 30 μ M. N.T. = Not tested. **Plaque reduction assays were performed against the M2-S31N containing A/WSN/33 virus in duplicates. The percent plaque formation is defined as the ratio of plaque numbers in the presence of compounds divided by the plaque numbers in the absence of compounds. *** CC_{50} values were determined using MDCK cells in the MTT assay. Δ clogP was calculated in ChemBioDraw Ultra 14.0.

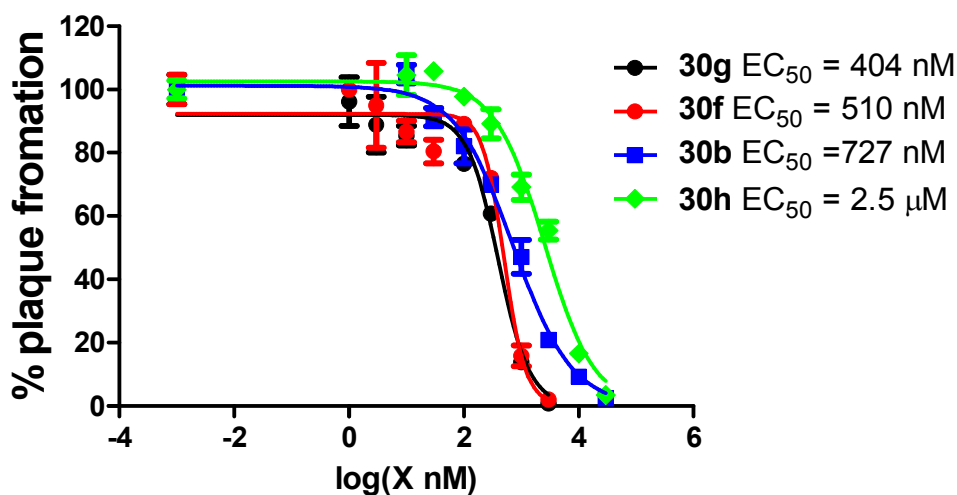


Figure 3. Antiviral activity of potent S31N inhibitors. Compounds are tested in duplicate with serial dilutions against A/WSN/33 (M2-S31N).

CONCLUSIONS

M2 belongs to a family of proteins called viroporins, which are virus-encoded ion channels.⁴²

Viroporins are involved in diverse steps during viral replication, including viral entry, assembly, and release. They are made of small (normally fewer than 100 amino acids), hydrophobic peptides by self-oligomerization and reside in the viral or cellular compartment membranes. Representative examples of viroporins include the hepatitis C virus p7 ion channel, the HIV vPu ion channel, M2 from the influenza virus, and the 6K proteins from alphavirus. Compounds that block cation flux through viroporins inhibit virus replication, corroborating viroporins as validated antiviral drug targets. The advantage of targeting viroporins compared to other viral proteins is that viroporins are relatively conserved, as one mutation causes multiple changes simultaneously in the constrained homo-oligomeric channel. For A/M2, only three predominant

1
2
3 drug-resistant mutations have been identified in transmissible viruses, namely V27A, L26F, and
4
5 S31N,^{19,20} all of which have similar levels of specific activity compared to the WT M2.⁴³
6
7

8
9 Starting from the lead compounds we identified earlier for S31N inhibition,^{27, 31} we hereby
10
11 disclose the SAR studies of the S31N inhibitor with the generic structure of adamantyl-1-
12
13 NH₂⁺CH₂-Aryl. The adamantane framework was found to be the optimal hydrophobic core,
14
15 suggesting that it fits snugly in the S31N channel. We next explored adding polar substitutions
16
17 to the adamantane framework to increase the drug-like properties of the compounds. Mono-
18
19 hydroxylation at the adamantane scaffold was well tolerated (compounds **30b**, **30f**, and **30g**).
20
21 Systematic substitutions of the heterocycle immediately attached to adamantane revealed that 1-
22
23 (1-adamantylamino)-methylene prefers to be placed at the 3 position of isoxazole and 1,3,4-
24
25 oxadiazole,²⁷ and the remaining variable 5 position favors hydrophobic substitutions, such as
26
27 alkyl, thienyl, and substituted phenyl. A wide variety of substitutions are tolerated at the *ortho*-,
28
29 *meta*-, and *para*-position of the distal ring when it is a phenyl group. Significantly, we have
30
31 identified several compounds (**26b** and **30f**) with much a higher selectivity index (relative to
32
33 toxicity towards mammalian cells) than the parent compound **4**. Collectively, the SAR agrees
34
35 with the mode of inhibitor binding inside the S31N channel,^{27,44} in which the adamantane ring is
36
37 surrounded by hydrophobic G34, the positively charged amine along with the heteroatom from
38
39 the first aryl ring forms bidentate hydrogen bonds with the N31 side chain amide, and the distal
40
41 aryl ring fits in the hydrophobic pocket formed by the V27 gate. The lead compounds identified
42
43 here have improved physical properties, and should provide excellent tools for in depth
44
45 pharmacological examinations.
46
47
48
49
50
51
52

53 54 55 **EXPERIMENTAL SECTION** 56 57 58 59 60

1
2
3 **Chemistry.** All chemicals are commercially available and were used without further purification.
4
5 Detailed synthesis procedures can be found in the Supporting Information for reactions described
6
7 in Schemes 1–4. All final compounds were purified by flash column chromatography, and the
8
9 purify of all compounds tested was $\geq 95\%$ as determined by LC-MS.
10
11

12
13 **Two-electrode voltage clamp (TEVC) assay.** The inhibitors were tested in a two-electrode
14
15 voltage clamp assay using *Xenopus laevis* frog oocytes microinjected with RNA expressing
16
17 either the WT or the S31N mutant of the A/M2 protein as previously reported.²⁹ The potency of
18
19 the inhibitors was expressed as percentage inhibition of A/M2 current observed after 2 min of
20
21 incubation with either 100 or 30 μM of compounds.
22
23

24
25 **Plaque reduction assay.** Plaque reduction assay was performed as previously reported.²⁷ The
26
27 viruses used for this assay were A/Udorn/72 and A/WSN/33, which contain WT and the S31N
28
29 mutant of M2, respectively.
30
31

32
33 **Cytotoxicity assay.** The cytotoxicity of compounds was determined using the CellTiter-Glo
34
35 Luminescent Cell Viability Assay kit from Promega. Briefly, Madin-Darby canine kidney
36
37 (MDCK) cells in DMEM + 10% FBS + P/S medium at 50,000 cells/mL were dispensed into
38
39 opaque 96-well plates (Cat #: CLS3362) at 100 μL /well. Twenty-four hours later, the growth
40
41 medium was replaced with fresh DMEM and compounds were added at two-fold series dilution
42
43 starting from 300 μM . After incubating for 72 h at 37 °C with 5% CO_2 in a CO_2 incubator, the
44
45 plates were equilibrated to room temperature before 100 μL of the CellTiter-Glo solution was
46
47 added. The plates were shaken for 5 s on a plate reader to allow even mixing. Luminescence
48
49 signals were recorded on a multimode SpectraMax M5 plate reader, and the signals were
50
51
52
53
54
55
56
57
58
59
60

1
2
3 normalized against the wells containing cells only. The CC_{50} values were calculated from best-fit
4
5 dose response curves with variable slope.
6
7

8 9 **ASSOCIATED CONTENT**

10 11 **Supporting information**

12
13
14
15 ^1H NMR, ^{13}C NMR, and mass spectrometry of intermediates and final products. This material is
16
17 available free of charge via the Internet at <http://pubs.acs.org>.
18
19

20 21 **AUTHOR INFORMATION**

22 23 24 **Corresponding Author**

25
26
27 Jun Wang, Tel: 520-626-1366, Fax: 520-626-0749, email: junwang@pharmacy.arizona.edu
28
29

30 31 **Notes**

32
33 The authors declare no competing financial interest.
34
35

36 37 **ACKNOWLEDGEMENTS**

38
39 This research is supported by NIH Grant AI119187 and the PhRMA foundation 2015 research
40
41 starter grant in pharmacology and toxicology to J.W. and NIH Grants GM056423 and AI74571
42
43 to W.F.D.
44
45

46 47 **ABBREVIATIONS USED**

48
49
50 WT, wild type; SAR, structure–activity relationship; DMEM, Dulbecco’s modified eagle
51
52 medium; MDCK, Madin-Darby Canine Kidney; TEV, two-electrode voltage clamps; HPAI,
53
54 highly pathogenic avian influenza; DAA, direct-acting antiviral.
55
56
57
58
59
60

REFERENCES

1. Cox, N.; Subbarao, K. Global epidemiology of influenza: Past and present. *Annu. Rev. Med.* **2000**, *51*, 407-421.
2. Thompson, W.; Shay, D.; Weintraub, E.; Brammer, L.; Cox, N.; Anderson, L.; Fukuda, K. Mortality associated with influenza and respiratory syncytial virus in the United States. *JAMA* **2003**, *289*, 179-186.
3. Thompson, W.; Shay, D.; Weintraub, E.; Brammer, I.; Bridges, C.; Cox, N.; Fukuda, K. Influenza-associated hospitalizations in the United States. *JAMA* **2004**, *292*, 1333-1340.
4. Osterholm, M.; Kelley, N.; Sommer, A.; Belongia, E. Efficacy and effectiveness of influenza vaccines: a systematic review and meta-analysis. *Lancet Infect. Dis.* **2012**, *12*, 36-44.
5. Lambert, L.; Fauci, A. Influenza Vaccines for the Future. *N. Engl. J. Med.* **2010**, *363*, 2036-2044.
6. Wong, S.; Webby, R. Traditional and New Influenza Vaccines. *Clin. Microbiol. Rev.* **2013**, *26*, 476-492.
7. Laursen, N. S.; Wilson, I. A. Broadly neutralizing antibodies against influenza viruses. *Antiviral Res.* **2013**, *98*, 476-483.
8. Pica, N.; Palese, P.; Caskey, C. Toward a Universal Influenza Virus Vaccine: Prospects and Challenges. *Annu. Rev. Med.* **2013**, *64*, 189-202.
9. Jin, H.; Chen, Z. Production of live attenuated influenza vaccines against seasonal and potential pandemic influenza viruses. *Curr. Opin. Virol.* **2014**, *6*, 34-39.
10. Qi, X.; Qian, Y. H.; Bao, C. J.; Guo, X. L.; Cui, L. B.; Tang, F. Y.; Ji, H.; Huang, Y.; Cai, P. Q.; Lu, B.; Xu, K.; Shi, C.; Zhu, F. C.; Zhou, M. H.; Wang, H. Probable person to person transmission of novel avian influenza A (H7N9) virus in Eastern China, 2013: epidemiological investigation. *BMJ* **2013**, *347*, f4752.
11. Preziosi, P. Influenza pharmacotherapy: present situation, strategies and hopes. *Expert Opin. Pharmacother.* **2011**, *12*, 1523-1549.
12. Webster, R. G.; Govorkova, E. A. Continuing challenges in influenza. *Annu. N. Y. Acad. Sci.* **2014**, *1323*, 115-139.
13. Wang, J.; Qiu, J. X.; Soto, C.; DeGrado, W. F. Structural and dynamic mechanisms for the function and inhibition of the M2 proton channel from influenza A virus. *Curr. Opin. Struct. Biol.* **2011**, *21*, 68-80.
14. De Clercq, E. Antiviral agents active against influenza A viruses. *Nat. Rev. Drug Discov.* **2006**, *5*, 1015-1025.
15. Hong, M.; DeGrado, W. F. Structural basis for proton conduction and inhibition by the influenza M2 protein. *Protein Sci.* **2012**, *21*, 1620-1633.
16. Davies, W. L.; Grunert, R. R.; Haff, R. F.; McGahen, J. W.; Neumayer, E. M.; Paulshock, M.; Watts, J. C.; Wood, T. R.; Hermann, E. C.; Hoffmann, C. E. Antiviral Activity of 1-Adamantanamine (Amantadine). *Science* **1964**, *144*, 862-863.
17. Pinto, L. H.; Holsinger, L. J.; Lamb, R. A. Influenza-Virus M2 Protein Has Ion Channel Activity. *Cell* **1992**, *69*, 517-528.
18. Dong, G.; Peng, C.; Luo, J.; Wang, C.; Han, L.; Wu, B.; Ji, G.; He, H. Adamantane-Resistant Influenza A Viruses in the World (1902–2013): Frequency and Distribution of M2 Gene Mutations. *PLoS ONE* **2015**, *10*, e0119115.
19. Furuse, Y.; Suzuki, A.; Kamigaki, T.; Oshitani, H. Evolution of the M gene of the influenza A virus in different host species: large-scale sequence analysis. *Virol. J.* **2009**, *6*, 67.

- 1
2
3
4
5
6
7
8
9
10
11
12
13
14
15
16
17
18
19
20
21
22
23
24
25
26
27
28
29
30
31
32
33
34
35
36
37
38
39
40
41
42
43
44
45
46
47
48
49
50
51
52
53
54
55
56
57
58
59
60
20. Furuse, Y.; Suzuki, A.; Oshitani, H. Large-scale sequence analysis of M gene of influenza A viruses from different species: mechanisms for emergence and spread of amantadine resistance. *Antimicrob. Agents Chemother.* **2009**, *53*, 4457-4463.
21. Wang, J.; Li, F.; Ma, C. Recent progress in designing inhibitors that target the drug-resistant M2 proton channels from the influenza A viruses. *Biopolymers* **2015**, *104*, 291-309.
22. Wang, J.; Ma, C.; Fiorin, G.; Carnevale, V.; Wang, T.; Hu, F.; Lamb, R. A.; Pinto, L. H.; Hong, M.; Kein, M. L.; DeGrado, W. F. Molecular Dynamics Simulation Directed Rational Design of Inhibitors Targeting Drug-Resistant Mutants of Influenza A Virus M2. *J. Am. Chem. Soc.* **2011**, *133*, 12834-12841.
23. Khurana, E.; Dal Peraro, M.; DeVane, R.; Vemparala, S.; DeGrado, W.; Klein, M. Molecular dynamics calculations suggest a conduction mechanism for the M2 proton channel from influenza A virus. *Proc. Natl. Acad. Sci. U S A* **2009**, *106*, 1069-1074.
24. Acharya, R.; Carnevale, V.; Fiorin, G.; Levine, B. G.; Polishchuk, A. L.; Balannik, V.; Samish, I.; Lamb, R. A.; Pinto, L. H.; DeGrado, W. F.; Klein, M. L. Structure and mechanism of proton transport through the transmembrane tetrameric M2 protein bundle of the influenza A virus. *Proc. Natl. Acad. Sci. U S A* **2010**, *107*, 15075-15080.
25. Stouffer, A. L.; Acharya, R.; Salom, D.; Levine, A. S.; Di Costanzo, L.; Soto, C. S.; Tereshko, V.; Nanda, V.; Stayrook, S.; DeGrado, W. F. Structural basis for the function and inhibition of an influenza virus proton channel. *Nature* **2008**, *452*, 596-599.
26. Wang, J.; Cady, S. D.; Balannik, V.; Pinto, L. H.; DeGrado, W. F.; Hong, M. Discovery of Spiro-Piperidine Inhibitors and Their Modulation of the Dynamics of the M2 Proton Channel from Influenza A Virus. *J. Am. Chem. Soc.* **2009**, *131*, 8066-8076.
27. Wang, J.; Wu, Y.; Ma, C.; Fiorin, G.; Wang, J.; Pinto, L. H.; Lamb, R. A.; Klein, M. L.; DeGrado, W. F. Structure and inhibition of the drug-resistant S31N mutant of the M2 ion channel of influenza A virus. *Proc. Natl. Acad. Sci. U S A* **2013**, *110*, 1315-1320.
28. Wang, J.; Ma, C.; Wu, Y.; Lamb, R. A.; Pinto, L. H.; DeGrado, W. F. Exploring organosilane amines as potent inhibitors and structural probes of influenza a virus M2 proton channel. *J. Am. Chem. Soc.* **2011**, *133*, 13844-13847.
29. Balannik, V.; Wang, J.; Ohigashi, Y.; Jing, X.; Magavern, E.; Lamb, R. A.; Degrado, W. F.; Pinto, L. H. Design and pharmacological characterization of inhibitors of amantadine-resistant mutants of the M2 ion channel of influenza A virus. *Biochemistry* **2009**, *48*, 11872-11882.
30. Wu, Y.; Canturk, B.; Jo, H.; Ma, C.; Gianti, E.; Klein, M. L.; Pinto, L. H.; Lamb, R. A.; Fiorin, G.; Wang, J.; DeGrado, W. F. Flipping in the Pore: Discovery of Dual Inhibitors that Bind in Different Orientations to the Wild-Type versus the Amantadine-Resistant S31N Mutant of the Influenza A Virus M2 Proton Channel. *J. Am. Chem. Soc.* **2014**, *136*, 17987-17995.
31. Wang, J.; Ma, C.; Wang, J.; Jo, H.; Canturk, B.; Fiorin, G.; Pinto, L. H.; Lamb, R. A.; Klein, M. L.; DeGrado, W. F. Discovery of Novel Dual Inhibitors of the Wild-Type and the Most Prevalent Drug-Resistant Mutant, S31N, of the M2 Proton Channel from Influenza A Virus. *J. Med. Chem.* **2013**, *56*, 2804-2812.
32. Schneider, J. W.; Gao, Z.; Li, S.; Farooqi, M.; Tang, T. S.; Bezprozvanny, I.; Frantz, D. E.; Hsieh, J. Small-molecule activation of neuronal cell fate. *Nat. Chem. Biol.* **2008**, *4*, 408-410.
33. McBriar, M. D.; Clader, J. W.; Chu, I.; Del Vecchio, R. A.; Favreau, L.; Greenlee, W. J.; Hyde, L. A.; Nomeir, A. A.; Parker, E. M.; Pissarnitski, D. A.; Song, L. X.; Zhang, L. L.; Zhao, Z. Q. Discovery of amide and heteroaryl isosteres as carbamate replacements in a series of orally active gamma-secretase inhibitors. *Bioorg. Med. Chem. Lett.* **2008**, *18*, 215-219.

- 1
2
3
4
5
6
7
8
9
10
11
12
13
14
15
16
17
18
19
20
21
22
23
24
25
26
27
28
29
30
31
32
33
34
35
36
37
38
39
40
41
42
43
44
45
46
47
48
49
50
51
52
53
54
55
56
57
58
59
60
34. Garfinkle, J.; Ezzili, C.; Rayl, T. J.; Hochstatter, D. G.; Hwang, I.; Boger, D. L. Optimization of the central heterocycle of alpha-ketoheterocycle inhibitors of fatty acid amide hydrolase. *J. Med. Chem.* **2008**, *51*, 4392-4403.
35. Cady, S. D.; Schmidt-Rohr, K.; Wang, J.; Soto, C. S.; DeGrado, W. F.; Hong, M. Structure of the amantadine binding site of influenza M2 proton channels in lipid bilayers. *Nature* **2010**, *463*, 689-692.
36. Corey, E. J.; Chaykovsky, M. Dimethyloxosulfonium Methylide ((CH₃)₂SOCH₂) and Dimethylsulfonium Methylide ((CH₃)₂SCH₂). Formation and Application to Organic Synthesis. *J. Am. Chem. Soc.* **1965**, *87*, 1353-1364.
37. Wang, J.; Ma, C.; Balannik, V.; Pinto, L. H.; Lamb, R. A.; DeGrado, W. F. Exploring the Requirements for the Hydrophobic Scaffold and Polar Amine in inhibitors of M2 from Influenza A Virus. *ACS Med. Chem. Lett.* **2011**, *2*, 307-312.
38. Duque, M. D.; Ma, C.; Torres, E.; Wang, J.; Naesens, L.; Juarez-Jimenez, J.; Camps, P.; Luque, F. J.; DeGrado, W. F.; Lamb, R. A.; Pinto, L. H.; Vazquez, S. Exploring the size limit of templates for inhibitors of the M2 ion channel of influenza A virus. *J. Med. Chem.* **2011**, *54*, 2646-2657.
39. Zhao, X.; Jie, Y.; Rosenberg, M. R.; Wan, J.; Zeng, S.; Cui, W.; Xiao, Y.; Li, Z.; Tu, Z.; Casarotto, M. G.; Hu, W. Design and synthesis of pinanamine derivatives as anti-influenza A M2 ion channel inhibitors. *Antiviral Res.* **2012**, *96*, 91-99.
40. Zhao, X.; Li, C.; Zeng, S.; Hu, W. Discovery of highly potent agents against influenza A virus. *Eur. J. Med. Chem.* **2011**, *46*, 52-57.
41. Hu, W. H.; Zeng, S. G.; Li, C. F.; Jie, Y. L.; Li, Z. Y.; Chen, L. Identification of Hits as Matrix-2 Protein Inhibitors through the Focused Screening of a Small Primary Amine Library. *J. Med. Chem.* **2010**, *53*, 3831-3834.
42. Nieva, J. L.; Madan, V.; Carrasco, L. Viroporins: structure and biological functions. *Nat. Rev. Micro.* **2012**, *10*, 563-574.
43. Balannik, V.; Carnevale, V.; Fiorin, G.; Levine, B.; Lamb, R.; Klein, M.; DeGrado, W.; Pinto, L. Functional Studies and Modeling of Pore-Lining Residue Mutants of the Influenza A Virus M2 Ion Channel. *Biochemistry* **2010**, *49*, 696-708.
44. Williams, J. K.; Tietze, D.; Wang, J.; Wu, Y.; DeGrado, W. F.; Hong, M. Drug-Induced Conformational and Dynamical Changes of the S31N Mutant of the Influenza M2 Proton Channel Investigated by Solid-State NMR. *J. Am. Chem. Soc.* **2013**, *135*, 9885-9897.

TOC

Influenza M2-S31N channel blockers

